COBEM 2023 27TH INTERNATIONAL CONGRESS OF MECHANICAL ENGENEERING

ABCM Brazilian Society of Mechanical Sciences and Engineering
27th ABCM International Congress of Mechanical Engineering
December 04-08, 2023, Florianópolis-SC, Brazil

COB-2023-0433
BACK-TO-BACK TEST RIG INSTRUMENTATION FOR TRANSMISSION ERROR MEASUREMENT

Matheus Fernandes Vieira
Guilherme José dos Santos
Ronnie Rodrigo Rego
Instituto Tecnológico de Aeronáutica
matheus.fernandes@ccm-ita.org.br[1]; guilherme@ita.br[2], ronnie@ita.br[3]

Abstract. *Gearbox noise emission has become a critical design factor for electric vehicles. The replacement of the internal combustion engine and the increased speed make the noise coming from the transmission more noticeable. Transmission error (TE) is the main source of excitation in a gearbox. The present work has as its objective sensoring a back-to-back test rig, and mapping the requirements, to measure TE. Two high precision incremental encoders have been used to measure the angular position of two shafts connected by a gear pair. TE was calculated by the difference between gear real and theoretical position. The experimental results were compared to those calculated with the help of KISSsoft. The gearbox dynamic behavior was also analyzed by monitoring the gearbox housing vibration. Test rig measurements for TE correlated well with KISSsoft calculations. Static transmission error proves to be an indicator of gearbox dynamics behavior. Encoders requirements to measure TE were mapped and evaluated. Regarding electric vehicle drivetrain systems, the presented approach is a tool for future investigations focused on improving NVH performance.*

Keywords: *transmission error, noise, vibration, instrumentation, electric powertrain*

1. INTRODUCTION

Electrification is a trend in the mobility industry. By 2022, 14% of cars sold worldwide were electric, while that figure was 9% in 2021 and 5% in 2020. Most of these sales occurred in three markets: China, Europe and the United States (IEA, 2023). China is the global leader of the electric vehicles (EV's) market and retains 60% of the EV's sales share. Projections show that EV's sales in China, United States and Europe will account for 40%, 20% and 25% of the vehicle market share, respectively, by 2030 (IEA, 2023). Moreover, investments are increasing not only in richer nations, but also in emerging countries. Government incentives are increasing both EV and automotive component manufacturing in India, Thailand and Indonesia (IEA, 2023). Emergence of new markets represents an increase in competitiveness, attracting new investments, reducing prices and financing new research.

The power transmission system is one of the challenges for the consolidation of electric vehicles. The reduced number of stages means that the gears operate at higher loads and speed, and have to withstand a greater number of cycles. As battery capacity is also a challenge, the electric motors have been scaled down to make them lighter. This strategy makes the engine reach speeds of up to 10,000 rpm to increase power capacity. Manufacturers have already announced the development of models capable of reaching 20,000 rpm and the projection is to reach 30,000 rpm by 2030 (Stadtfeld, 2020). These operating conditions entail various obstacles regarding noise, vibration and harshness (NVH) performance. Gears meshing at high speed generate strange high-pitched humming sounds (Stadtfeld, 2020). As the electric motor is quieter than the internal combustion engine, this sound poses a problem for noise comfort and safety.

The most significant sources of noise in a gearbox are classified as rattle and whine noise. Rattle occurs due to torque fluctuations that cause the idling gears to collide with each other in circumferential backlash (Morello et al, 2011). This type is not the main concern in EV's because their motors deliver smooth torque (Palermo et al., 2018). The whine noise comes from transmission error (TE), which is the angular deviation between the actual wheel position and its expected position based on the pinion angular position. TE is calculated by

$$TE_\theta = \theta_g - \frac{\theta_p * N_p}{N_g}, \tag{1}$$

where θ_g is the gear displacement, θ_p is the pinion displacement, N_p is the pinion number of teeth and N_g is the gear number of teeth.

Equation (1) gives TE in angular units. However, it's more common to express TE in the form of linear displacement along the line of action, given by

$$TE = r_{bg} * \left(\theta_g - \frac{\theta_p * N_p}{N_g}\right), \quad (2)$$

where r_{bg} is the base radius of the gear.

In a gear with perfect involute form and perfectly rigid teeth, TE would not occur (Smith, 2003). However, in real gears, speed variation caused by TE generates oscillations that are transferred along adjacent structures. Once the vibration meets a thin outer surface, such as the gearbox case, it causes a variation in air pressure, generating noise (Smith, 2003).

Thus, transmission error is widely used to predict NVH performance of gearboxes and provides information for gear tooth and body optimization. It is generally classified into three types: dynamic transmission error (DTE), manufacturing transmission error (MTE) and static transmission error (STE) (Palermo et al., 2018). Although DTE is more closely related to gear vibration, its prediction is complex and so STE is used to improve NVH performance as it excites DTE (Tharmakulasingam, 2009).

The most established method to measure transmission error is by using angular encoders (Palermo et al., 2018). Interpolation is used to extract high precision position information from encoders. This technique is very powerful because it allows you to measure very low displacements without the need to increase the number of slits of the encoder. However, it is important to note that this increased precision is limited by the interpolation resolution of the sensor, according to its calibration chart.

The present work has as its objective mapping the sensors' requirements and instrumenting a back-to-back test rig to measure TE. An experimental plan was designed to perform the tests and the repeatability of the method shall be verified. The gear platform calculation KISSsoft was used as reference to evaluate the measurements. Correlation between peak-to-peak transmission error (PPTE) and gearbox acceleration was developed.

2. MATERIALS AND METHODS

The equipment used in the work was the ITA's back-to-back test rig. It is designed to perform gear tests on different gear geometries with torque up to 250 Nm and speeds up to 5,000 rpm. The equipment monitors torque, oil level and temperature, vibration and speed, ensuring safety and the accuracy of the tests. Figure 1 shows a representation of the ITA's test rig. The Test Box 71 was used to conduct the tests in this work.

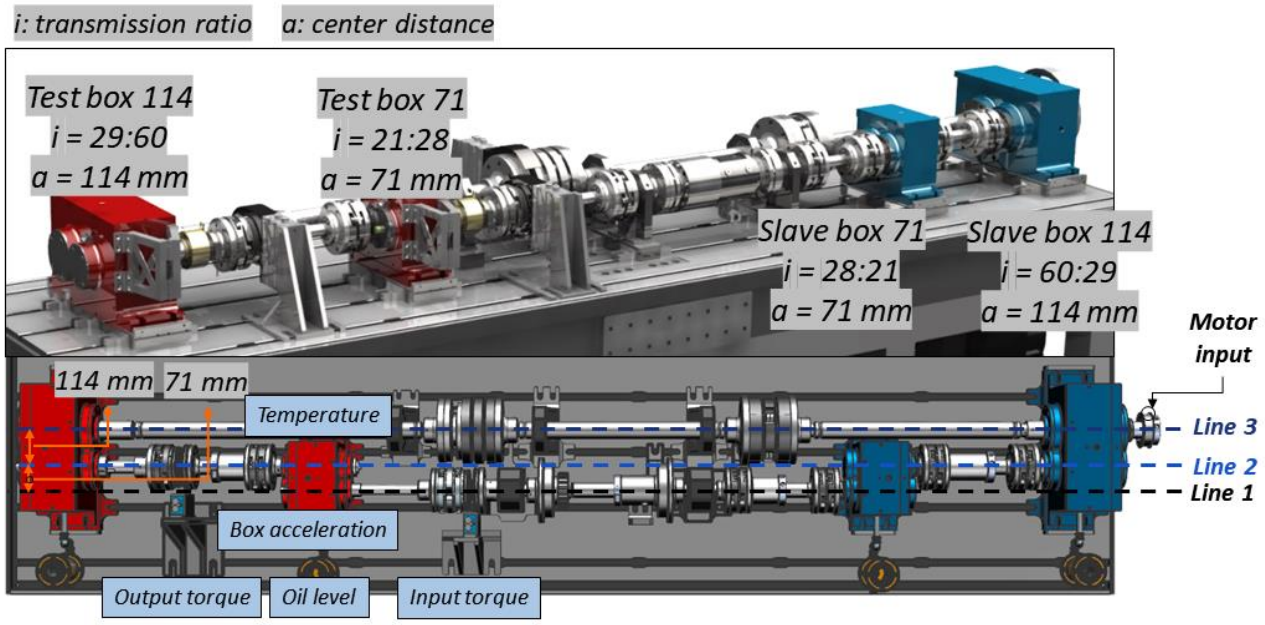

Figure 1. ITA's back-to-back test rig.

To define the requirements for TE measurement, it was previously calculated in the gear platform calculation KISSsoft. The Weber/Banaschek approach was used to estimate tooth stiffness. From this, tooth deflection was calculated and used with profile modification to obtain transmission error. Stiffness modelling was carried out for different loads to understand gear response at different torque levels. Figure 2 presents the main gear pair parameters as well as the simulated TE obtained with the help of KISSsoft.

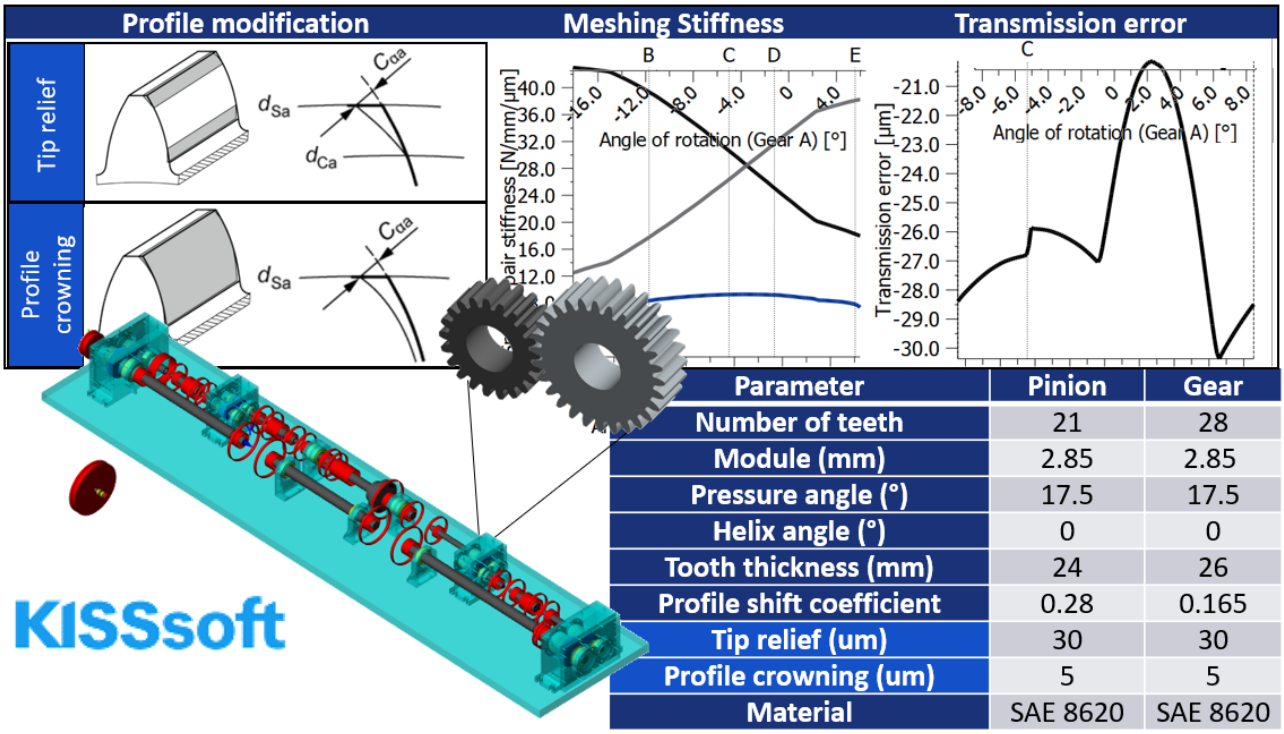

Parameter	Pinion	Gear
Number of teeth	21	28
Module (mm)	2.85	2.85
Pressure angle (°)	17.5	17.5
Helix angle (°)	0	0
Tooth thickness (mm)	24	26
Profile shift coefficient	0.28	0.165
Tip relief (um)	30	30
Profile crowning (um)	5	5
Material	SAE 8620	SAE 8620

Figure 2. Transmission error calculation in KISSsoft and gear pair parameters.

The magnitude order of TE in the designed gear was obtained from the simulations in KISSsoft. The smaller amplitude (TE_{min}) was taken to guarantee accuracy of the measurement for any load condition. To accurately describe the phenomenon's, frequency Nyquist theorem states that a sampling frequency of at least twice that of the phenomenon is needed (Balbinot and Brusamarello, 2010). Considering Nyquist theorem and Eq. (2), the maximum resolution allowed for the encoder can be found by

$$RES = \frac{0.5 * TE_{min}}{r_{bg} + r_{bp}}, \tag{3}$$

where r_{bp} is the base radius of the pinion.

The chosen encoder model was the Heidenhain ERA 4400, which corresponds to a sine-cosine optical encoder. The chosen drum has 6,000 slits along its outer diameter, which provides high accuracy. The sensor outputs two sinusoidal signals phase-shifted by 90º. It allows a slit to be divided into four quadrants of the trigonometric circle, making it possible to measure smaller displacements by dividing the outer diameter into 24,000 parts. In addition to dividing each slit into four, it is possible to interpolate the signal within each quadrant through a tangent interpolation. Figure 3 explains the interpolation procedure, which was used to further increase measurement resolution according to:

$$\theta = \frac{360°}{4 * 6{,}000} * \left(P + \frac{arctan\left(\frac{A}{B}\right)}{90°} \right), \tag{4}$$

where P is the number of pulses in the waveform output, A is the signal from the sine channel and B is the signal from the cosine channel.

Palermo et al. (2018) calculates the minimum required number of points in a revolution dividing 2π by RES. From the number of points and shaft speed the required sampling frequency can be calculated. Applying Nyquist theorem, the minimum sampling rate is defined by

$$sr_{min} = \frac{2 * N * RPM}{60}, \tag{5}$$

where N is the number of points, RPM is the shaft speed in revolution per minute.

Increasing the number of divisions indistinctly will result in a false measurement once the sensor has its intrinsic error and is not able to measure such small magnitude. The maximum number of points in an encoder revolution is defined by

$$N_{max} = \frac{2\pi}{\epsilon}, \tag{6}$$

where ϵ is the maximum error of the encoder according to its calibration chart.

Given the number of points and the sampling rate, it is necessary to use an acquisition system capable of collecting and storing a high amount of data in a short period of time. To meet the requirements, a NI7962-R FPGA (field-programmable gate array) module from National Instruments was used. This device has four channels with a sampling frequency of 120 MS/s each, ±2 V peak-to-peak voltage input and 16-bit resolution. Equation (7) shows the required resolution, in bits, for the analog-to-digital converter:

$$RES_{bits} = log_2{}^{RES-1}. \tag{7}$$

After the sensors and data acquisition system were defined, encoders were installed in the test rig, one on the pinion shaft of Test Box 71 and another on the gear shaft of the same gearbox. The mounting tolerances of the sensors are very tight and a mechanical device was designed to provide the necessary precision for mounting the sensors. Figure 3 shows the encoders in the test rig and the device installed.

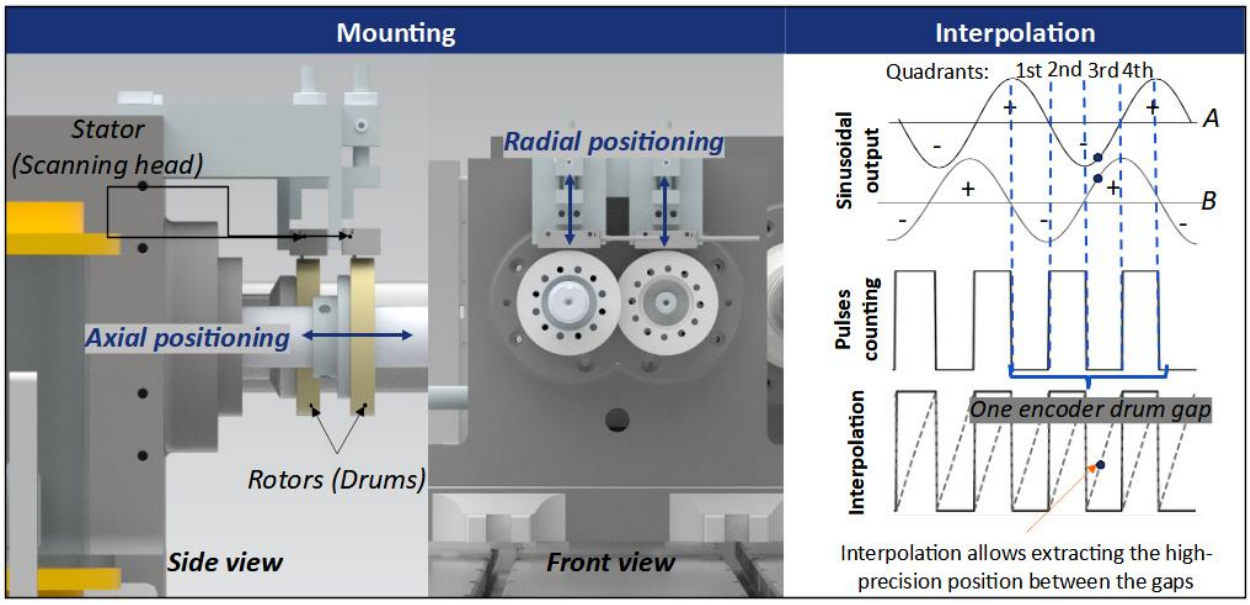

Figure 3. Sensors' mounting and interpolation technique.

During the tests, three gear pairs with the same geometry were used to ensure repeatability. For each torque level on each gear pair, 3 replications were performed, resulting in 63 runs in total. Table 1 summarizes the inputs and outputs of the first part of the DoE.

Table 1. DoE for STE measurement.

	Factors			Responses
Treatment	Torque (Nm)	Replication	Gear	STE
1 to 63	0 to 180, with step of 30	3	3	One curve for each treatment

In the second part of the DoE, velocity was analyzed to evaluate the dynamic response and correlate it with the STE. A wide range of operating conditions was investigated. For each torque level, speed was varied from 125 to 4000 rpm, providing a total of 224 runs. After repeatability being validated in the first part of the DoE, a single gear was used in the second part of the DoE. The result of this part was the measured acceleration in the gearbox housing. Table 2 summarizes the input and outputs of the second part of the DoE.

Table 2. DoE for dynamic behavior evaluation.

	Factor		Responses
Treatment	Speed (rpm)	Torque (Nm)	Gearbox housing acceleration
1 to 224	125 to 4000, step of 125	20 to 180, step of 20	One curve for each treatment

After collecting the experimental data, signal processing analyses were conducted with the relevant Python 3 libraries *numpy*, *scipy*, *pandas* and *matplotlib*.

3. RESULTS AND DISCUSSIONS

Figure 4 shows PPTE simulation results for different torque levels. The minimum PPTE value to be measured according to the simulations were 3.88 µm, and thus, it was used as a reference for the encoder specification. Applying Eq. (3), the maximum resolution allowed to measure TE considering Nyquist theorem is 5.13×10^{-5} rad. Heidenhain ERA 4400 has a measuring step of 2.64×10^{-4} rad, and when combined with interpolation, it can achieve higher resolutions. The calibration chart of the sensor informs that the maximum position error of the sensor is 4.09×10^{-6} rad.

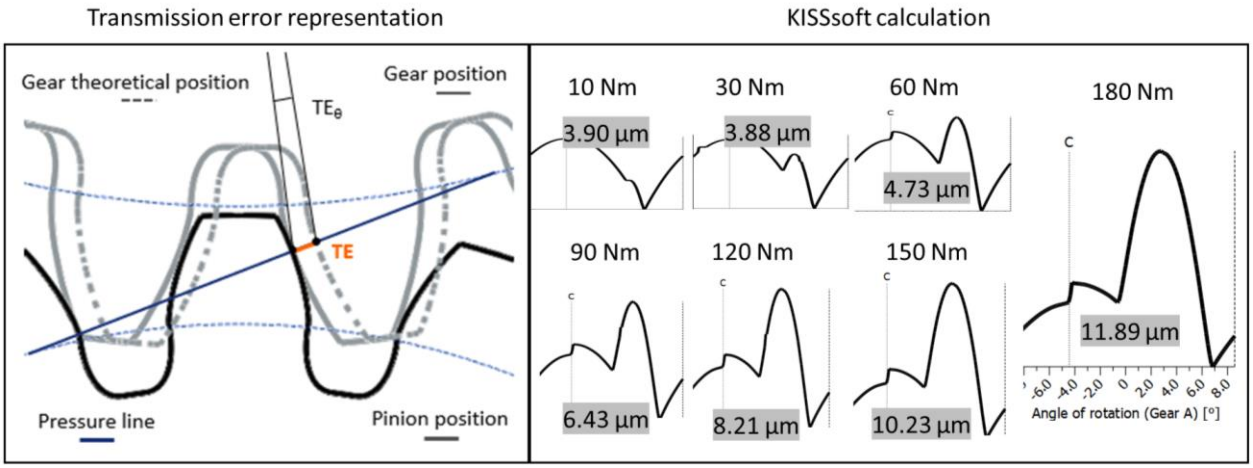

Figure 4. Peak-to-peak transmission error calculated in KISSsoft for different torques.

In the first part of the DoE, a speed of 60 rpm was used. Considering the calculated resolution, it takes 123,245 divisions per revolution to measure TE. Following Eq. (5), a minimum sampling rate of approximately 120,000 points per second would be required. A common practice to reduce signal aliasing is to use a sampling rate of 10 times the phenomenon frequency. Therefore, a sampling rate of 960 kS/s was used.

As ERA 4400 provides a continuous output, it may not be necessary to acquire an elevated amount of data to extract high precision position information. To apply the interpolation technique, it is necessary to have at least one point inside each quadrant. When the quadrant is identified, the fine precision position is extracted interpolating the voltage signal. As there are 24,000 quadrants in a revolution, this principle would give a much smaller sampling rate, of 48 kS/s according to Nyquist theorem.

During the tests, the voltage signal from each encoder displayed some amount of noise. A significant component of the noise had its origin mapped to the test rig motor by acquiring data from the encoders while the motor was turned off and observing the noise levels. The signal-to-noise ratio was significantly improved with the help of a band-pass filter. Once the encoder signal has 6,000 periods per revolution, for a shaft speed of 60 rpm (1 Hz), the output data has a frequency of 6,000 Hz for the pinion as shown in Figure 5. The data coming from the encoder was centered around 6,000 Hz and this band was taken from the signal. The signal frequency lower than the low frequency cut-off and higher than the high frequency cut-off defined in Figure 5 were removed. Applying the inverse FFT, it could be seen that the noise was mitigated.

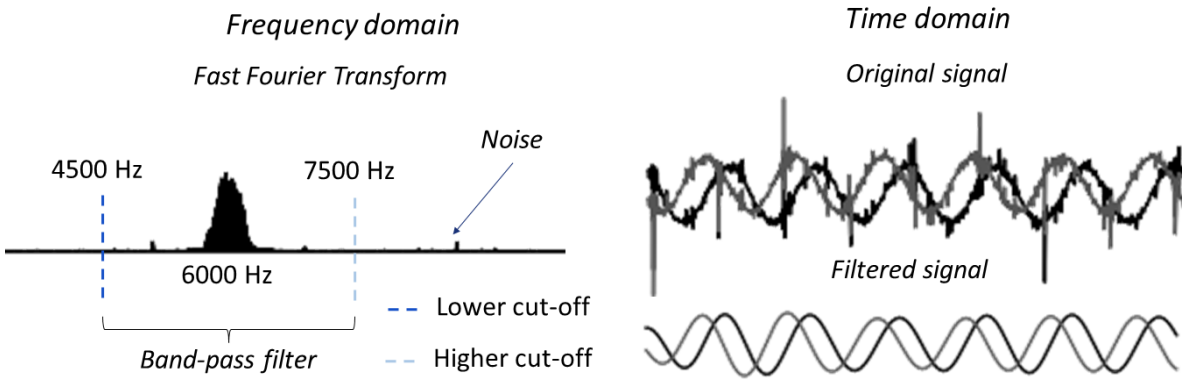

Figure 5. Encoder signal processing.

With the band-pass filter defined, the minimum sampling rate was evaluated. Different decimation factors were applied to the original signal and the TE calculated from the down sampled signals were compared. A t-test was performed to compare the mean of peak-to-peak transmission error of the data samples. Since the hunting tooth period (HTP) of the gear is four revolutions, the mean peak-to-peak for 4 revolutions was considered. The box-plot in Figure 6 presents a comparison between TE calculated with a sampling rate of 960 kS/s, 120 kS/s, 48 kS/s and 24 kS/s. From Figure 6, the TE calculated from the signal with 24 kS/s shows a much broader interquartile range compared with the results for the first three sampling rates.

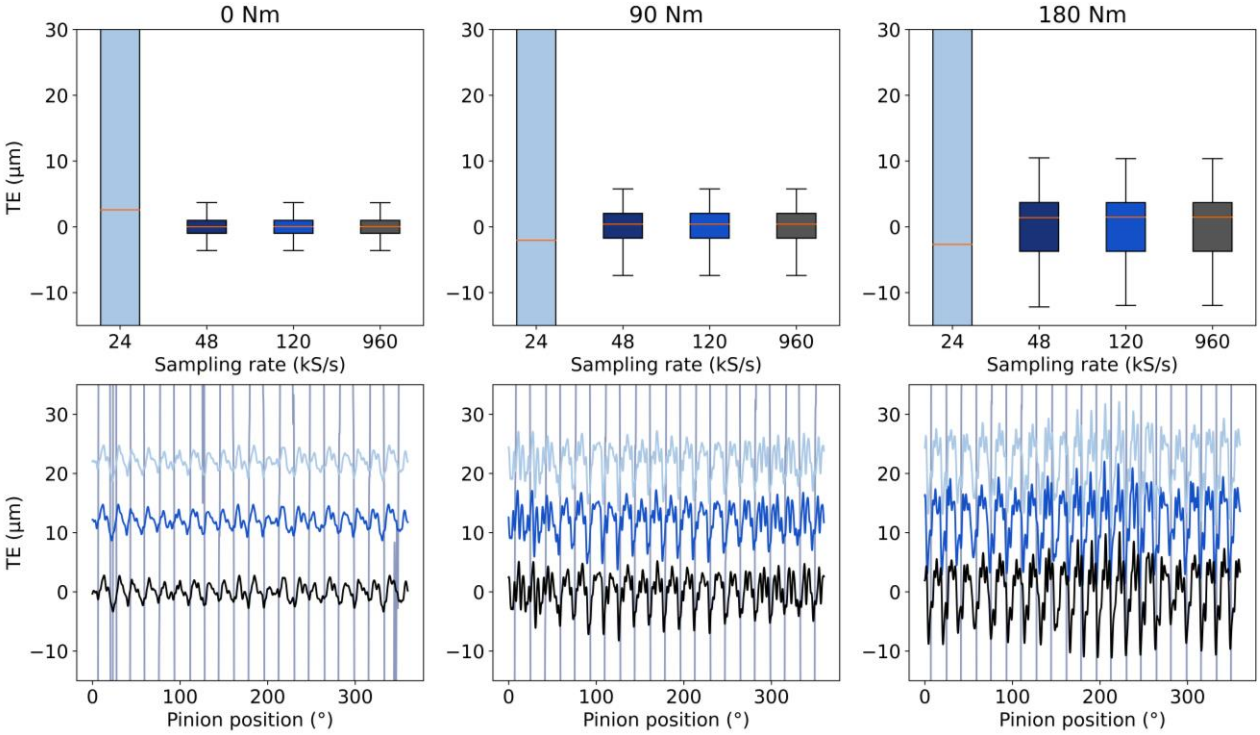

Figure 6. Box-plot and signal in time domain of TE calculated by different sampling rates and torques. Below, a DC shift was added to TE curve for 24 kS/s, 48 kS/s and 120 kS/s to ease visualization.

Taking the mean of PPTE in four revolutions and considering a significance level of 95%, the null hypothesis $u_1 = u_2$ could be accepted for 120 kS/s and 48 kS/s, but it was rejected for 24 kS/s in t-test. Therefore, the analysis was performed considering a sampling rate of 48 kS/s, reducing time processing and memory usage by approximately 95%. This represents a reduction of 23,75 GB and 4793 seconds on a computer equipped with 32 GB RAM, an SSD and an Intel i7 2.50 GHz processor.

Looking at the frequency domain of transmission error for each condition, it was possible to identify the shaft rotation and gear mesh frequency, as shown in Figure 7. The amplitude of each component of STE varied according to the applied

torque. It was observed that the amplitude of MTE remained the same for all torque levels, since it depends on only the manufacturing.

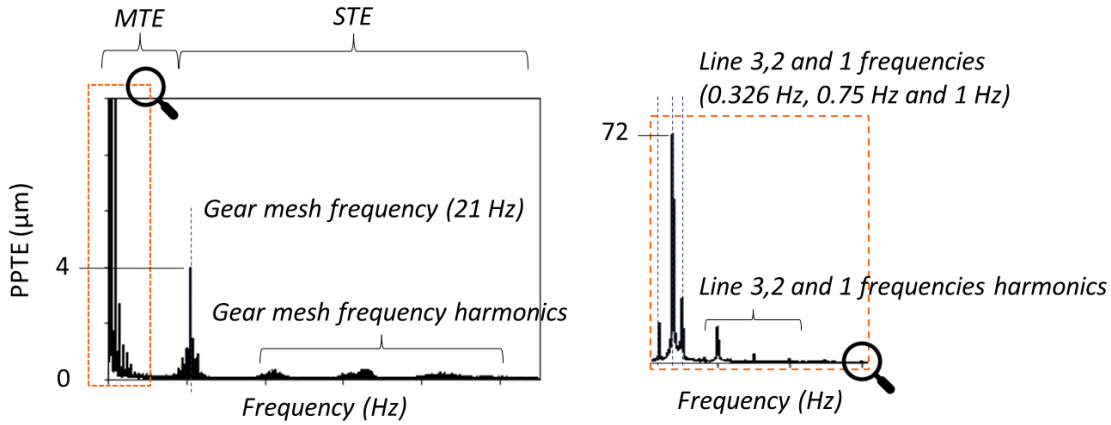

Figure 7. Frequency response of transmission error and MTE and STE identification.

The repeatability of the developed method was evaluated comparing the results obtained in each replication and for each gear. A t-test was applied following the same conditions. Considering a significance level of 95%, the null hypothesis was accepted for all replications in all gears, confirming the repeatability. An interesting observation is that one of the three gears tested presented a peak in one tooth for low loads. Following the observations of Chin et al. (2020), it was possibly caused by tooth wear or manufacturing deviation, since it does not manifest in high loads, probably because of superposition of elastic deflection. Figure 8 shows the STE curve for gear 1 subjected to two different torques.

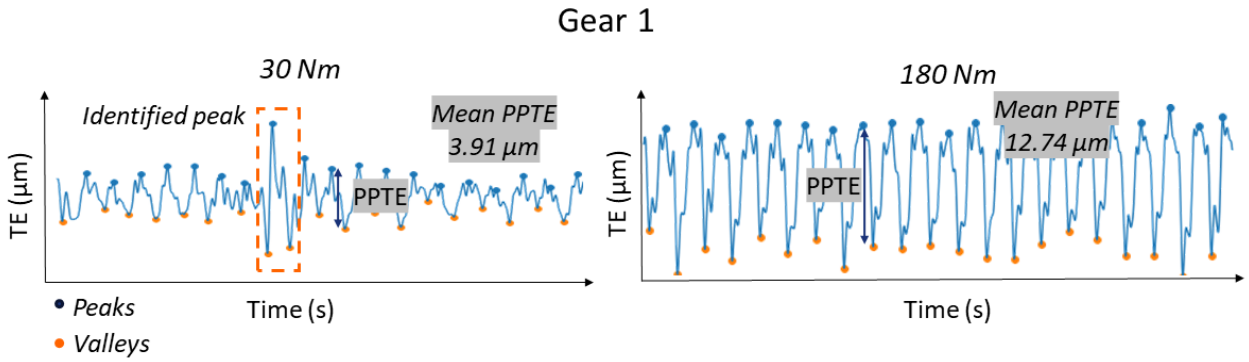

Figure 8. Peak identification in STE curve for low torques in Gear 1.

Figure 9a shows the comparison between transmission error obtained in the experiments with those calculated in KISSsoft. In low torques, the measured result corresponded exactly with the calculated one. For high torques, despite the similar behavior, the absolute value showed some discrepancies. Flek et. al (2021) observed stiffness super estimation in the analytical approach in comparison with Finite Element Method (FEM). This observation can explain the similarities observed for low torques, where the deflection is minima and the discrepancies for high torques, where the deflection increases. Another important observation is that the calculations were made using the designed microgeometry, not the measured one. Bihr et al. (2015) observed significant differences between TE calculated using these two conditions.

Once the experimental results approximated well the analytical method, the comparison between transmission error and dynamic behavior of the gearbox was analyzed. Higher vibrations are expected for higher transmission errors and it was evaluated in the tests. Figure 9b shows the acceleration components of the gearbox housing for different torques. There are high vibration components in the gear meshing frequency for high torques at high speeds. Taking a speed of 4000 rpm as an example, the gear mesh frequency is 1400 Hz and its equivalent peak is highlighted in Figure 9b.

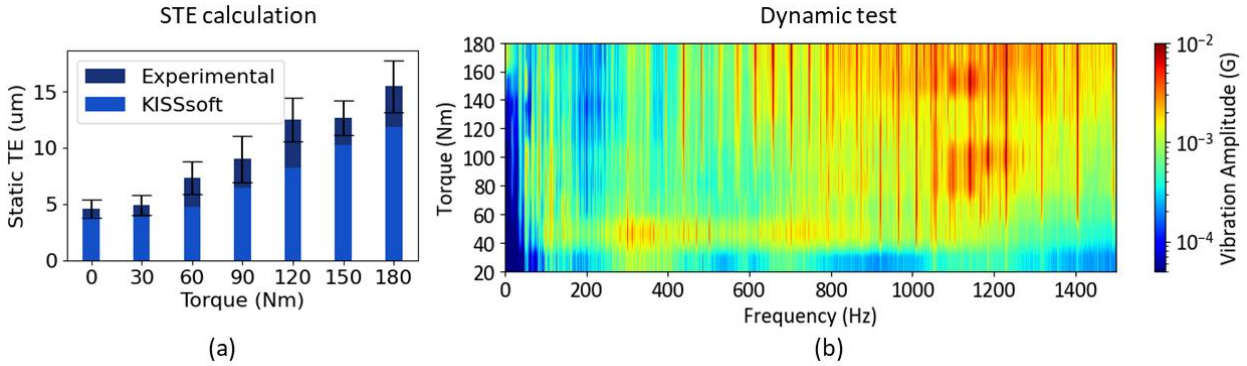

Figure 9. (a) Comparison between experimental and calculated STE. (b) Gearbox housing acceleration for different operating conditions.

The expected relation between STE and gearbox acceleration was obtained. An R-value of 0.97 for the two variables was calculated. It means that STE have a big influence on the dynamic response of the gearbox. For higher STE, higher will be the vibration in the gearbox, behavior was also observed by Palermo et al. (2018).

4. CONCLUSIONS

The work allowed the understanding of angular encoders requirements to measure transmission error. It was observed that the analogue output was essential to achieve the objective of the work. Not only the sampling rate is important, but specially the encoder measuring error and the resolution of the analogue-digital data converter. This allows the interpolation technique to extract very precise position information from the encoder shafts, reducing memory usage and processing time by 95%.

Another important conclusion is that the method showed high repeatability. For all replications in all gears, the results were statistically the same according to t-test for a 95% confidence level. It was also possible to observe tooth irregularities analyzing transmission error in the time domain.

Regarding the comparison between transmission error calculated in KISSsoft and the obtained experimentally, a good approximation was achieved. The same components in FFT were observed in both and transmission error increased for higher torques in both. Amplitude differences in high loads can be hitched to super estimation of stiffness in analytical approach.

At last, the expected correlation between static transmission error and gearbox case vibration was validated. This observation supports the consistency of the developed method, allowing it to be used in further research to improve NVH performance in gearboxes. It also supports STE as an indicator of gearbox dynamic behavior.

5. ACKNOWLEDGMENTS

I would like to thank Instituto Tecnológico de Aeronáutica (ITA) and Centro de Competência em Manufatura (CCM-ITA) for the infrastructure and the opportunity to develop this work. I would also like to thank Fundep for the financial incentives in the form of research scholarship.

6. REFERENCES

Balbinot, A. and Brusamarello, V., 2010. Instrumentação e Fundamentos de Medidas, Vol. 1. Editor LTC.

Bihr, J, Heider, M., Otto, M., Stahl, K., Kume, T., Kato, M., 2015. *Gear Noise Prediction in Automotive Transmissions.* International Gear Conference, held in Lyon, 26th-28th August, 2014.

Chin, Zhan Yie, et al. 2020. “Absolute transmission error: A simple new tool for assessing gear wear”. Mechanical Systems and Signal Processing. 11 June 2020, p. 15.

Flek J, Dub M, Kolář J, Lopot F, Petr K, 2021. “Determination of Mesh Stiffness of Gear—Analytical Approach vs. FEM Analysis”. Applied Sciences. 28 May 2021; 11(11):4960.

IEA. *Global EV Outlook 2023*. 2023. Available at: https://www.iea.org/reports/global-ev-outlook-2023. Accessed at: 05 June 2023.

Morello, L., Rossini, L., Pia, G., Tonoli, A., 2011. The Automotive Body: Volume II. Editor Springer.

Palermo, A., Britte, L., Janssens, K., Mundo, D., Desmet, W., 2018. “The measurement of Gear Transmission Error as an NVH indicator: Theoretical discussion and industrial application via low-cost digital encoders to an all-electric vehicle gearbox”. Mechanical Systems and Signal Processing. Volume 110, p. 368-389.

Smith, J., 2003. Gear noise and vibration. Editor CRC Press.

Stadtfeld, H., 2020. *Introduction to electric vehicle transmissions*. Gear Technology, 37(7), 42-50, 2020.
Tharmakulasingam, R., 2009. *Transmission Error in Spur Gears: Static and Dynamic Finite-Element Modeling and Design Optimization.* Doctor's thesis, School of Engineering and Design, Brunel University, United Kingdom.

7. RESPONSIBILITY NOTICE

The authors are the only responsible for the printed material included in this paper.